Journal of Molecular Histology (2020) 51:33–46
https://doi.org/10.1007/s10735-019-09854-8

ORIGINAL PAPER

Disruption of tight junction structure contributes to secretory dysfunction in IgG4-related sialadenitis

Sai-Nan Min[1] · Li-Ling Wu[2] · Yan-Yan Zhang[1] · Wen-Xuan Zhu[1] · Xin Cong[2] · Guang-Yan Yu[1]

Received: 27 October 2019 / Accepted: 10 December 2019 / Published online: 21 December 2019

Abstract

IgG4-related sialadenitis (IgG4-RS) is a chronic fibro-inflammatory disease characterized by swelling of salivary glands and varying degrees of xerostomia. Tight junctions (TJs) play an essential role in maintaining secretory function by regulating the paracellular flow of ions and water. However, whether TJs are altered and contribute to the hyposecretion in IgG4-RS is not fully understood. Here, a total of 399 differentially expressed proteins were identified in IgG4-RS submandibular glands (SMGs) and enriched in the regulation of actin cytoskeleton and the salivary secretion. Real-time PCR results showed that the mRNA levels of claudin-3, -4, -6, -7, -8, -10, -12, occludin, and ZO-1 were significantly lower, whereas claudin-1 and -5 were higher in IgG4-RS SMGs. Immunohistochemical and immunofluorescence staining revealed that claudin-1, -3, -4, occludin, and ZO-1 were mainly distributed at apicolateral membranes in acini and ducts of SMGs from controls, whereas claudin-1 protein intensity at apicolateral membrane was elevated, while the staining of claudin-3, -4, and ZO-1 were reduced in IgG4-RS SMGs. Occludin was dispersed into cytoplasm of acini and ducts in SMGs of patients. Among them, claudin-3 and ZO-1 protein levels were positively correlated with saliva flow rate. Furthermore, the decreased fluorescence intensity of F-actin at peri-apicolateral membranes and the loss of ZO-1 staining at the same location were observed in acinar and ductal cells of IgG4-RS SMGs, which might be responsible for disorganization of TJ complex. Taken together, these findings indicate that the integrity of TJ complex of SMGs is impaired and might contribute to hyposalivation of IgG4-RS patients.

Keywords Tight junction · F-actin · IgG4-related sialadenitis · Hyposalivation

Introduction

IgG4-related disease (IgG4-RD) is a chronic fibro-inflammatory condition involving multiple organs, including the pancreas, salivary gland, lacrimal gland, bile duct, kidney, lung, artery, and skin, which were previously recognized as individual disease entities (Umehara et al. 2014). The hallmark features of IgG4-RD are enlargement of the affected organs, extensive infiltration of $IgG4^+$ plasma cells, and storiform fibrosis. The involvement of salivary gland is observed in 27% to 58% of IgG4-RD patients, known as IgG4-related sialadenitis (IgG4-RS), which is characterized by swelling and stiffness of single or multiple salivary glands with varying degrees of xerostomia (Brito-Zeron et al. 2014; Stone et al. 2012; Liu et al. 2019). The histopathological characteristics include acinar atrophy, prominent cellular interlobular fibrosis, and dense lymphocyte and plasma cell infiltration. Previous study has reported that 81% IgG4-RS patients have a mild to moderate reduction in saliva flow rate at rest, and ^{99m}Tc-pertechnetate scintigraphy shows that the secretion index of submandibular gland (SMG) is lower than the normal value in 77.4% IgG4-RS patients (Li et al. 2015b). Based on the severity of inflammation and fibrosis, the stimulated saliva flow rate decreases as the histopathological grade increases (Li et al. 2015b). Therefore, exploring the underlying mechanism involved in the hyposecretion

✉ Xin Cong
congxin@bjmu.edu.cn

✉ Guang-Yan Yu
gyyu@263.net

[1] Department of Oral and Maxillofacial Surgery, Peking University School and Hospital of Stomatology, National Engineering Laboratory for Digital and Material Technology of Stomatology, Beijing 100081, People's Republic of China

[2] Department of Physiology and Pathophysiology, Peking University School of Basic Medical Sciences, Key Laboratory of Molecular Cardiovascular Sciences, Ministry of Education, and Beijing Key Laboratory of Cardiovascular Receptors Research, Beijing 100191, People's Republic of China

of IgG4-RS is of great importance for understanding the pathogenesis of IgG4-RS and finding a novel therapeutic strategy.

Tight junctions (TJs) are intercellular junctional complexes that regulate the transport of water, ions, and solutes through paracellular pathway in epithelia and endothelia. TJs are composed of more than 40 different proteins, which can be divided into transmembrane proteins such as claudins and occludin, and cytosolic components like zonula occludens-1 (ZO-1) (Baker 2016). In SMGs, TJs play an indispensable barrier role in the paracellular transport of different sized molecules, and herein determine the amount and composition of the secreted saliva (Forster 2008; Zhang et al. 2013). Notably, the integrity of TJ proteins in salivary gland epithelium are vulnerable to be impaired under pathological conditions, including genetic predisposition, immune disorder, and exposure to environmental stress (Buckley and Turner 2018; Krug et al. 2014). For example, the expression of ZO-1 and occludin are decreased, while claudin-1 and -4 are increased and redistributed from apical to basolateral membranes in labial salivary glands from patients with Sjögren's syndrome, another autoimmune disease characterized by lymphocytic infiltration and hyposecretion of exocrine glands (Ewert et al. 2010). Loss of ZO-1 is also observed in SMGs from xerostomia patients who received head and neck radiation therapy (Nam et al. 2016). In addition, we previously found that in a rabbit long-term model of SMG autotransplantation, which is an effective surgical therapy to treat severe dry eye syndrome, the acinar muscarinic acetylcholine receptors (mAChRs) are hypersensitive and contribute to hypersecretion by inducing the opening of TJ-based paracellular pathway and the accumulation of filamentous actin (F-actin) at peri-apicolateral membranes (Yang et al. 2017). Moreover, in epiphora patients who underwent partial gland reduction after SMG autotransplantation, the mRNA and protein expressions of ZO-1 and occludin are increased, whereas the interaction between them is decreased in the transplanted SMGs (Ding et al. 2017). These findings imply that the abnormality of TJs is an important mechanism that causes dysfunction in salivary glands. Hence, whether TJs are altered and related with xerostomia in IgG4-RS are worth to be determined.

In IgG4-related cholangitis patients, Th2 cytokines open the paracellular pore pathway by increasing claudin-2 expression, resulting in the disruption of the barrier function of biliary epithelial cells (Muller et al. 2013). The expression and distribution of claudin-4, -7, occludin, and junctional adhesion molecule-A are unaltered in the ductal epithelium of SMGs derived from IgG4-RS patients (Abe et al. 2016). However, it is still unclear whether the expression and distribution of TJs alter in both acini and ducts of SMGs from IgG4-RS patients and contribute to the alteration in salivary secretion. Therefore, the present study was designed to detect the changes of TJs in SMGs derived from IgG4-RS patients, and further analyze the relationship and possible mechanism between TJs and the progression of IgG4-RS.

Materials and methods

Reagents and antibodies

Primary antibodies against claudin-1 (BS6778), claudin-3 (BS1067), and claudin-4 (BS1068) were purchased from Bioworld Technology (Minnesota, MN, USA). Antibody against ZO-1 (617300), Alexa Fluor-594-conjugated occludin antibody (331594) and Alexa Fluor-594-conjugated secondary antibody (R37119) were from Thermo Fisher Scientific.

Patients and biopsy specimens

A total of 22 individuals (20 to 74 years old, 10 men) diagnosed as IgG4-RS according to the comprehensive diagnostic criteria (Umehara et al. 2012) were recruited in this study (Table 1). SMGs collected from 15 individuals who underwent neck dissection for primary tongue squamous carcinoma, which were pathologically confirmed normal, were enrolled as control (Table 2). All patients had signed an informed consent form following protocol approved by the Ethics Committee of Peking University School and Hospital of Stomatology (No. PKUSSORB-2013008). Immediately after surgery, the part of specimens was frozen in liquid nitrogen for the extraction of protein and RNA, and the remaining part was embedded for immunohistochemical and immunofluorescence experiments. The whole saliva was collected at rest for 5 min and the saliva flow rate was calculated as described previously (Li et al. 2015b).

iTRAQ sample preparation

Six frozen SMG tissues (3 IgG4-RS and 3 controls) were homogenized on ice, and 100 μg of homogenates from each were used for proteomic screening. Protein lysate was obtained using lysis buffer (7 mol/L urea, 2 mol/L thiourea, 0.1% CHAPS, and protease inhibitor cocktail) followed by centrifugation at 15,000×*g* for 1 h at 4 °C to remove cellular debris. Protein concentration was detected using Bradford assay. The protein samples were digested with trypsin solution (80 μg/mL) overnight at 37 °C and labeled with iTRAQ reagents (AB Sciex, Redwood City, CA, USA) according to

Table 1 Clinical characteristics and serological findings of patients with IgG4-related sialadenitis (IgG4-RS)

No	Age	Sex	Swollen glands				Saliva flow rate at rest (g/5 min)	Complications	$IgG4^+$ cells (/HPF)	Serological findings				
			LG	PG	SMG	SLG				SS-A/Ro	SS-B/La	IgG (g/L)	IgG4 (g/L)	IgE (KU/L)
1	63	M	+	+	+	−	6.362	−	119	−	−	18.3	N/A	79.84
2	50	F	+	−	+	−	4.483	Allergic rhinitis	110	−	−	N/A	4.89	202
3	55	M	−	−	+	+	N/A	−	54	−	−	489.2	3.43	55
4	61	F	+	+	+	−	N/A	Asthma, SC	148	−	−	28.62	35.6	1656
5	74	M	+	−	+	+	0.1	Allergic rhinitis, SC	86	−	-	21.08	12.3	45.6
6	28	F	+	−	+	−	N/A	−	82	−	−	26.4	5	637
7	60	M	−	−	+	−	N/A	−	89	−	−	20	4.04	371.4
8	62	M	+	−	+	−	1.427	−	88	−	−	N/A	5.36	N/A
9	67	F	−	−	+	+	N/A	Asthma, AIP	134	−	−	29.16	21.7	242
10	70	M	+	−	+	−	N/A	Hypertension	52	−	−	N/A	6.54	2226
11	56	F	−	−	+	+	N/A	−	56	−	−	15	3.61	76.71
12	61	F	+	+	+	+	N/A	AIP	126	−	−	20.1	7.23	273.1
13	55	F	+	+	+	−	N/A	−	114	−	−	15.2	6.5	703.4
14	65	M	+	−	+	+	N/A	−	102	−	−	25.9	32.9	877.7
15	47	M	+	+	+	−	N/A	−	132	−	−	17.4	15	925.6
16	62	M	+	+	+	−	N/A	AIP	95	−	−	33.07	25.5	1618
17	47	F	+	−	+	+	0.53	SC	78	−	−	13.98	7.21	408
18	51	F	+	+	+	+	N/A	Arthritis	126	−	−	13.51	11.7	1023
19	50	F	+	+	+	+	0.45	−	195	−	−	14.77	9.11	53
20	20	F	−	−	+	−	0.41	−	60	−	−	13.3	2.14	5.3
21	47	M	+	+	+	−	5.78	AIP	124	−	−	18.84	13.8	N/A
22	53	F	−	−	+	+	0.0975	−	90	−	−	15.13	3.23	1143

AIP autoimmune pancreatitis, *HPF* high power field, *LG* lachrymal gland, *LSG* labial salivary gland, *N/A* not available, *PG* parotid gland, *SC* sclerosing cholangitis, *SLG* sublingual gland, *SMG* submandibular gland, + positive, − negative

Table 2 Clinical characteristics of patients enrolled as control

No	Age	Sex	Diagnosis
1	56	Male	Tongue carcinoma
2	67	Male	Tongue carcinoma
3	57	Female	Tongue carcinoma
4	54	Female	Tongue carcinoma
5	72	Female	Tongue carcinoma
6	65	Male	Tongue carcinoma
7	71	Female	Tongue carcinoma
8	61	Male	Tongue carcinoma
9	56	Male	Tongue carcinoma
10	46	Female	Tongue carcinoma
11	42	Female	Tongue carcinoma
12	61	Male	Tongue carcinoma
13	66	Female	Tongue carcinoma
14	40	Male	Tongue carcinoma
15	61	Female	Tongue carcinoma

the manufacturer's instructions. Then, the six labeled samples were pooled, centrifuged, and dried.

Liquid chromatography-tandem mass spectrometry (LC–MS/MS)

Sample was analyzed using an EASY-Spray analytical column (120 mm × 75 μm, 3 μm) on an EASY-nLC1000 connected to a Q Exactive mass spectrometer (Thermo Fisher Scientific, Beverly, MA, USA). Peptides were eluted by using a binary solvent system with 99.9% H_2O, 0.1% formic acid (phase A) and 99.9% acetonitrile, 0.1% formic acid (phase B). The following linear gradient was used: 5–8% B in 13 min, 8–30% B in 77 min, 30–50% B in 10 min, 50–95% B in 5 min, washed at 95% B for 10 min. The eluent was introduced directly to a Q-Exactive mass spectrometer via EASY-Spray ion source. Source ionization parameters were as follows: capillary temperature, 320 °C, spray voltage, 2.3 kV, and declustering potential, 100 V. For data-dependent acquisition MS runs, one full scan MS (Automatic Gain Control target of 3e6 or 20 ms injection time) from 300 to 1800 m/z followed by 20 MS/MS scans (Automatic Gain Control target 1e5 or 120 ms injection time) were continuously acquired. The resolution for MS was set to 70,000 and for MS/MS was set to 17,500. For higher energy collisional dissociation, the normalized collision energy of 32% was applied.

Quantitative real-time PCR

Total RNAs were extracted from homogenized SMG tissues by using Trizol (Invitrogen, Carlsbad, CA, USA) according to the manufacturer's instructions. cDNA was synthesized with the RevertAid First Strand cDNA Synthesis Kit (Promega, Madison, WI, USA) and amplified using DyNAmoTM ColorFlash SYBR Green qPCR kit (Thermo Fisher Scientific) under a PikoReal Real-Time PCR System (Thermo Fisher Scientific). The primers used for TJs and GAPDH were listed in Table 3.

Western blot analysis

Total proteins were extracted from SMG tissues by RIPA lysis buffer (Thermo Fisher Scientific) with protease inhibitors (Roche, Basel, Switzerland), and the protein concentration was measured by the Bradford method. Equal amounts

Table 3 Primers for human tight junction components mRNA

Gene	Upper primer (5′–3′)	Lower primer (5′–3′)	Size (bp)
Claudin-1	GCAGAAGATGAGGATGGCTGT	CCTTGGTGTTGGGTAAGAGGT	253
Claudin-2	GCCATGATGGTGACATCCAGT	TCAGGCACCAGTGGTGAGTAG	218
Claudin-3	GGACTTCTACAACCCCGTGGT	AGACGTAGTCCTTGCGGTCGT	230
Claudin-4	CAAGGCCAAGACCATGATCGT	GCGGAGTAAGGCTTGTCTGTG	246
Claudin-5	GGCACATGCAGTGCAAAGTGT	ATGTTGGCGAACCAGCAGAGT	247
Claudin-6	GGTGCTCACCTCTGGGATTGT	GCAGGGGCAGATGTTGAGTAG	267
Claudin-7	CTCGAGCCCTAATGGTGGTCT	CCCAGGACAGGAACAGGAGAG	326
Claudin-8	CCGTGATGTCCTTCTTGGCTTTC	CTCTGATGATGGCATTGGCAACC	176
Claudin-9	GGTACACTGGGCACCTGTGAT	GCTTCGACCGGCTTAGAACTG	312
Claudin-10	CTGTGGAAGGCGTGCGTTA	CAAAGAAGCCCAGGCTGACA	132
Claudin-11	CTGATGATTGCTGCCTCGGT	ACCAATCCAGCCTGCATACAG	243
Claudin-12	AGTCACTGCTCCCGTCATACC	TTCTGAATCTGGCCCAAGTCT	250
Occludin	CTTCGCCTGTGGATGACTTC	CTTGCTCTGTTCTCTTTGACCTT	117
ZO-1	CCTTCAGCTGTGGAAGAGGATG	AGCTCCACAGGCTTCAGGAAC	287
GAPDH	ACATCATCCCTGCCTCTACTG	CCTGCTTCACCACCTTCTTG	180

ZO-1 zonula occludens-1

of the protein (30 μg) were separated on 12% SDS-PAGE and transferred to polyvinylidene difluoride membranes. The membranes were blocked with 5% nonfat milk, probed with primary antibodies at 4 °C overnight, and then incubated with anti-mouse or anti-rabbit horseradish peroxidase (HRP)-conjugated secondary antibodies (Zhongshan Laboratories, Beijing, China) at room temperature. Immunoreactive bands were detected by enhanced chemiluminescence reagent (Thermo Fisher Scientific Pierce, Rockford, IL, USA). Image J Software (National Institutes of Health, Bethesda, MD, USA) was used to quantify the densities of bands.

Immunohistochemical and immunofluorescence staining

SMG tissues were fixed in formalin, embedded in paraffin and cut into consecutive sections (5 μm). For immunohistochemical staining, sections were stained with primary antibodies against claudin-1 and -3 at 4 °C overnight, and then incubated with HRP–conjugated secondary antibodies (Zhongshan Laboratories) at 37 °C for 2 h. Five randomly chosen fields from each section were captured under a light microscope (Q550CW, Leica, Wetzlar, Germany). For immunofluorescence, specimens were blocked with 1% bovine serum albumin, incubated with antibodies against claudin-4, occludin, and ZO-1 at 4 °C overnight and then incubated with Fluor-594-conjugated secondary antibodies at 37 °C for 2 h. For the staining of F-actin, sections were incubated with FITC-phalloidin (Sigma-aldrich, St. Louis, MO, USA) at 37 °C for 2 h. Nuclei were stained with 4,6-diamidino-2-phenylindole (DAPI). Fluorescence images were captured under confocal microscope (Leica TCS SP8).

Statistical analysis

Data were normalized and shown as mean ± SEM. Statistical analysis was performed by unpaired Student's *t* test between IgG4-RS and control groups using GraphPad software (GraphPad Prism 6.01, San Diego, CA, USA). Correlation was analyzed by Pearson's coefficient correlation analysis. *P* value less than 0.05 was considered statistically significant.

Results

Clinical characteristics of IgG4-RS patients

Clinical features, serologic examinations, and secretion function of IgG4-RS patients were summarized in Table 1. Among 22 patients included in this study, 10 were males and 12 were females with a ratio of 1:1.2. The mean ages of patients were 54.73 ± 12.54 years. The level of IgG4 was elevated in 21 cases in whom the serum concentration of IgG4 was measured (> 1.35 g/L). The serum IgE level was increased in 14 of 20 (70%) subjects. The unstimulated saliva flow rate of 9 IgG4-RS patients was 2.182 ± 2.594 g/5 min (range from 0.097 to 6.362 g/5 min). The great variation of saliva flow rate suggested that the secretory function was aberrant with varying degrees in IgG4-RS patients.

Alteration of protein profiles in SMGs from IgG4-RS patients

To screen the changes of protein profiles in IgG4-RS, we compared the SMG samples derived from 3 patients and 3 controls by using iTRAQ labeling and LC–MS/MS. A total of 399 differentially expressed proteins were identified according to ratios of fold-change (≥ 1.5 or ≤ 0.66, $P < 0.05$), of which 272 were upregulated and 127 were downregulated (Fig. 1a). Based on the differentially expressed proteins, Kyoto Encyclopedia of Genes and Genomes (KEGG) pathway enrichment analysis was performed. The top 15 enriched pathways from KEGG analysis were shown in Fig. 1b, including leukocyte transendothelial migration, Fc gamma R-mediated phagocytosis, B cell receptor signaling pathway, antigen processing and presentation, etc. Notably, as red arrows pointed out, most of the identified differentially expressed proteins were involved in the regulation of actin cytoskeleton. The dynamic interaction between cytoskeleton and TJ proteins played a crucial role in coordinating the process of salivary secretion, which was also enriched by KEGG analysis on the differentially expressed proteins. Hence, the screening results provided an intriguing hint that TJ proteins, which are linked with actin cytoskeleton and the secretory function, might be changed in IgG4-RS SMGs.

Alteration of TJ mRNA expressions in SMGs from IgG4-RS patients

We then performed real-time PCR to examine the mRNA levels of claudin-1 ~ 12, occludin, and ZO-1 in SMG specimens. As shown in Fig. 2, the mRNA expression of claudins, including claudin-3, -4, -6, -7, -8, -10, and -12, occludin, and ZO-1 were significantly lower in IgG4-RS SMGs compared with those in control group ($P < 0.05$ or $P < 0.01$), claudin-1 and -5 levels were markedly elevated ($P < 0.05$ or $P < 0.01$), while claudin-2, -9, and -11 levels were not changed. These results showed that the transcriptional levels of TJs were changed in IgG4-RS SMGs.

Alteration of TJ distribution and protein expressions in SMGs from IgG4-RS patients

In addition to mRNA expression, the distribution with proper protein content of TJs at the apicolateral membranes

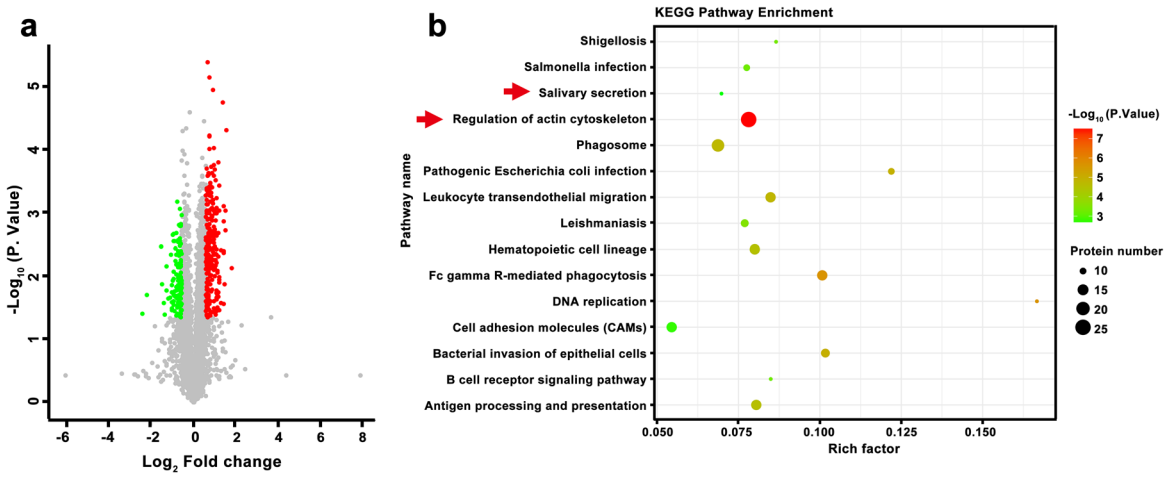

Fig. 1 The alteration of protein profile in submandibular glands from IgG4-related sialadenitis (IgG4-RS) patients. **a** Volcano plot displaying the log 2 fold change for proteomics data (*x*-axis) and log 10 *P* value (*y*-axis). The red points and the green points represented proteins that were significantly upregulated (ratio ≥ 1.5) and downregulated (ratio ≤ 0.67) in IgG4-RS patients, respectively. **b** The Kyoto Encyclopedia of Genes and Genomes (KEGG) pathway enrichment analysis of the differentially expressed proteins showing the top 15 enriched pathways

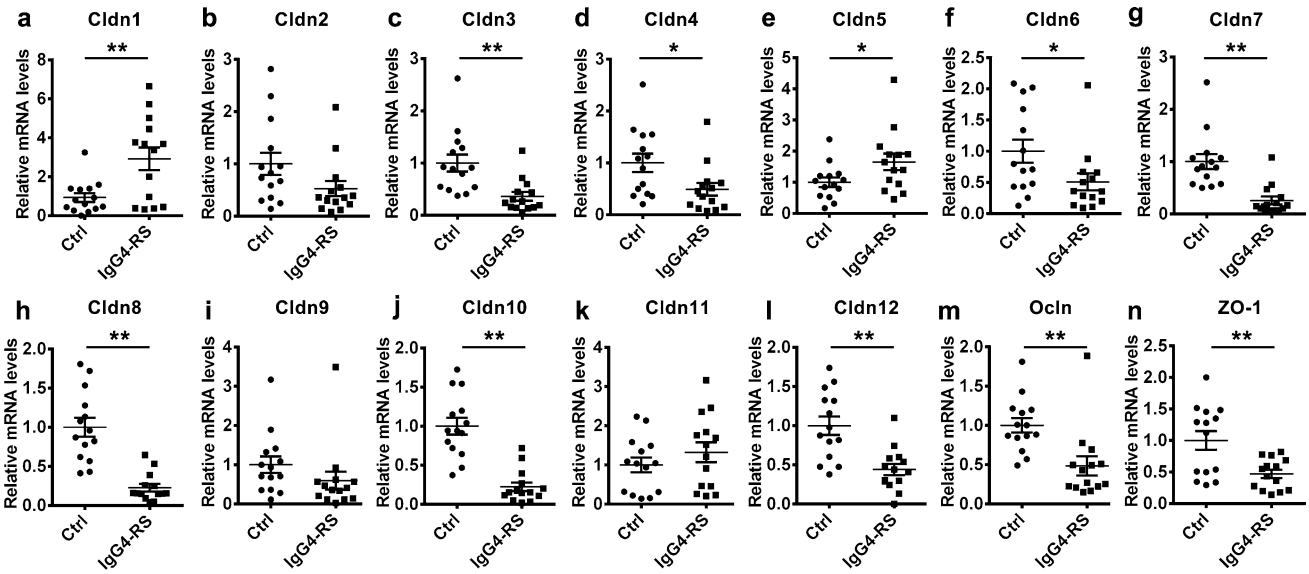

Fig. 2 Alteration of tight junction (TJ) mRNA expressions in submandibular glands from IgG4-related sialadenitis (IgG4-RS) patients compared with controls. The mRNA levels of claudin-1 to -12 (**a**–**l**), occludin (**n**) and zonula occludens-1 (**o**) measured by real time-PCR in patients (n = 14) and controls (n = 14) were shown. All data are presented as mean ± SEM. *Cldn* claudin, *Ctrl* control, *Ocln* occludin, *ZO-1* zonula occludens-1. **P* < 0.05 and ***P* < 0.01 compared with controls

are crucial factors that guarantee their barrier function (Barrera et al. 2013). Accordingly, we detected the distribution of claudin-1, -3, -4, occludin, and ZO-1, the five major TJ components in human, rat, and mouse SMGs, by immunohistochemical or immunofluorescence staining and also measured their protein expressions by western blot analysis.

Compared with control group, the acinar and ductal cells of SMGs from IgG4-RS patients underwent morphologic alteration accompanied by increased lymphocytic infiltration and fibrosis. In areas without prominent lymphocytic infiltration, acini became atrophic with preserved morphology. However, in dense lymphocytic infiltration zone, destruction of acini and fibrosis around acinar and ductal cells were noted (Fig. 3a). Therefore, we observed the changes of TJ components under mild and severe lymphocytic infiltration, respectively. In acini of control SMGs, claudin-1 was mainly localized at the apicolateral and basal membranes (as arrows shown in Fig. 3b). In

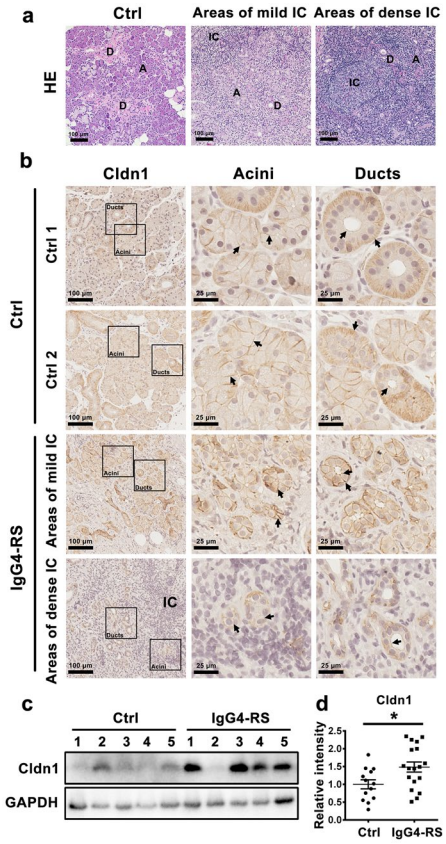

Fig. 3 Distribution and protein expression of claudin-1 in submandibular glands (SMGs) from IgG4-related sialadenitis (IgG4-RS) patients and controls. **a** Histological morphology of SMGs from IgG4-RS patients and controls by hematoxylin–eosin staining. **b** The immunohistochemical staining of claudin-1 in acini and ducts of SMGs. The areas with mild and dense inflammatory cells infiltrates were both observed in SMGs from IgG4-RS patients. Cell nuclei were stained with hematoxylin. Arrows pointed to the claudin-1-specific staining. The enlarged images were derived from the black boxes. *A* acini, *D* duct, *IC* infiltrating cells. **c, d** The protein expression and quantitative analysis of claudin-1 in SMGs from IgG4-RS patients (n = 18) and controls (n = 13). All data are presented as mean ± SEM. *Cldn* claudin, *Ctrl* control, *HE* hematoxylin–eosin staining. $^{*}P < 0.05$ compared with controls

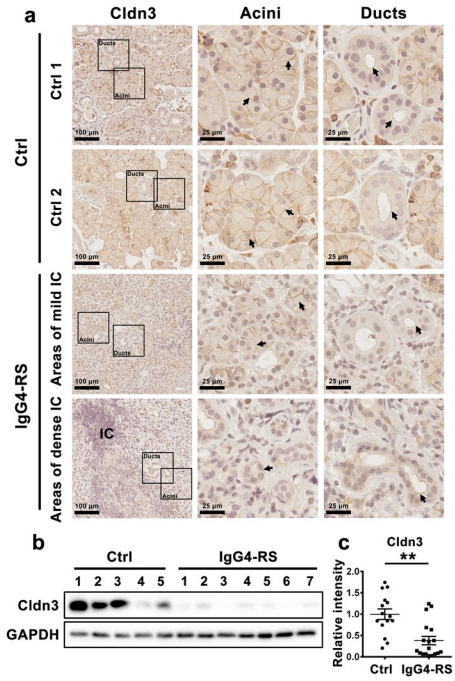

Fig. 4 Distribution and protein expression of claudin-3 in submandibular glands (SMGs) from IgG4-related sialadenitis (IgG4-RS) patients and controls. **a** The immunohistochemical staining of claudin-1 in acini and ducts of SMGs. The areas with mild and dense inflammatory cells infiltrates were both observed in SMGs from IgG4-RS patients. Cell nuclei were stained with hematoxylin. Arrows pointed to the claudin-3-specific staining. The enlarged images were derived from the black boxes. *A* acini, *D* duct, *IC* infiltrating cells. **b, c** The protein expression and quantitative analysis of claudin-3 in SMGs from IgG4-RS patients (n = 18) and controls (n = 15). All data are presented as mean ± SEM. *Cldn* claudin, *Ctrl* control. $^{**}P < 0.01$ compared with controls

the areas with mild lymphocytic infiltration, the staining intensity of claudin-1 was increased at both apicolateral and basal membranes in acini of IgG4-RS SMGs, while the staining intensity of claudin-1 became weak around lymphocytic infiltration foci. In the ductal cells of control SMGs, claudin-1 was predominantly presented at the basolateral membranes and extended to the basal infoldings of cells. In IgG4-RS SMGs, claudin-1 was redistributed to both basolateral and apical plasma membranes with an enhanced staining intensity in ducts distal to lymphocytic infiltration foci, concomitant with the disappearance of basal infoldings in ductal cells. However, for ducts close to abundant inflammatory cell infiltrates, the staining intensity of claudin-1 became decreased and discontinuous (as arrows shown in Fig. 3b). In order to assess the changes in total protein level in lesions, western blot was performed and results showed that the protein level of claudin-1 was significantly increased in IgG4-RS patients ($P < 0.05$, Fig. 3c, d).

In acini of SMGs from the controls, claudin-3 staining was observed at the apicolateral and basal plasma membranes, a phenomenon similar to claudin-1. However, in IgG4-RS patients, the reduction of claudin-3 staining was observed in acini, and the staining was almost disappeared in dense lymphocytic infiltration zone (as arrows shown in Fig. 4a). Moreover, in ducts of control SMGs, claudin-3 was localized at the apicolateral membranes with an intensity which was weaker than that in acini. The distribution and staining intensity of claudin-3 were unaltered in ducts of SMGs from IgG4-RS patients, in areas with either less or dense lymphocytic infiltration (as arrows shown in Fig. 4a). Consistently, western blot results confirmed that

the protein level of claudin-3 was significantly decreased in SMGs of IgG4-RS patients compared with control tissues ($P < 0.01$, Fig. 4b, c).

The localization of claudin-4 in acinar and ductal cells of control SMGs were mainly expressed at the apical and basolateral plasma membranes including basal infoldings (Fig. 5a). In areas with mild lymphocytic infiltration in IgG4-RS SMGs, the intensity of claudin-4 was reduced at plasma membranes of acinar cells, while in ductal cells, no obvious change of claudin-4 was observed. Notably, in areas with lymphoid aggregates, claudin-4 was predominantly expressed in both plasma membranes and cytoplasm of acinar and ductal cells with decreased intensity. Western blot showed that the total protein level of claudin-4 was also lower in IgG4-RS patients ($P < 0.01$, Fig. 5b, c).

In acinar and ductal cells of SMGs from control subjects, occludin was distributed continuously at the apicolateral plasma membranes (Fig. 6a). However, in the residual acini and ducts of SMGs from IgG4-RS patients, the staining of occludin became discontinuous and redistributed into cytoplasm as multiple dots, but the distribution showed no difference with the increase of infiltrating lymphocytes (Fig. 6a). Western blot results showed that the protein level of occludin was significantly increased in SMGs of IgG4-RS patients ($P < 0.01$, Fig. 6b, c), which was in accordance with the elevated staining intensity in acinar and ductal cytoplasm as shown above.

Similar with occludin, ZO-1 was mainly located at the apicolateral membranes in both acinar and ductal cells of control SMGs. By contrast, the intensity at the apical membranes was markedly reduced in the acini and ducts of IgG4-RS patients, and the staining of ZO-1 was even weaker in dense lymphocytic infiltration zone (Fig. 7a). Western blot analysis further showed the consistent results with a lower ZO-1 protein expression in SMGs from IgG4-RS patients ($P < 0.05$, Fig. 7b, c). Collectively, these above results indicated that the structure and expression of TJ complex were impaired in SMG lesions of IgG4-RS patients.

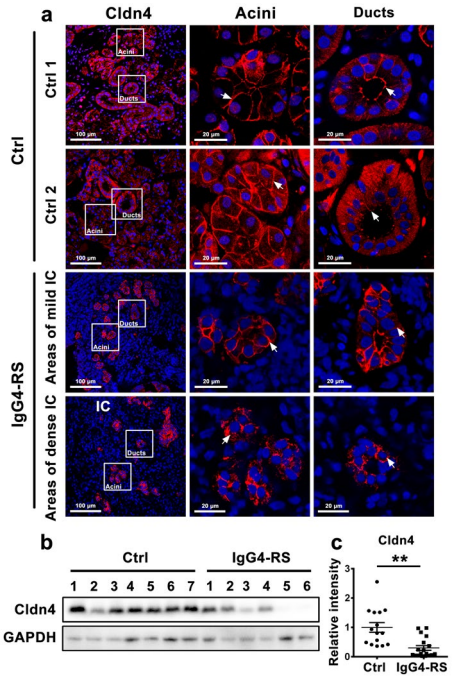

Fig. 5 Distribution and protein expression of claudin-4 in submandibular glands (SMGs) from IgG4-related sialadenitis (IgG4-RS) patients and controls. **a** The immunofluorescence staining of claudin-4 in acini and ducts of SMGs. The areas with mild and dense inflammatory cells infiltrates were both observed in SMGs from IgG4-RS patients. Cell nuclei were stained with DAPI (blue). Arrows pointed to the claudin-4-specific staining. The enlarged images were derived from the black boxes. *A* acini, *D* duct, *IC* infiltrating cells. **b, c** The protein expression and quantitative analysis of claudin-4 in SMGs from IgG4-RS patients (n = 18) and controls (n = 15). All data are presented as mean ± SEM. *Cldn* claudin, *Ctrl* control. $^{**}P < 0.01$ compared with controls

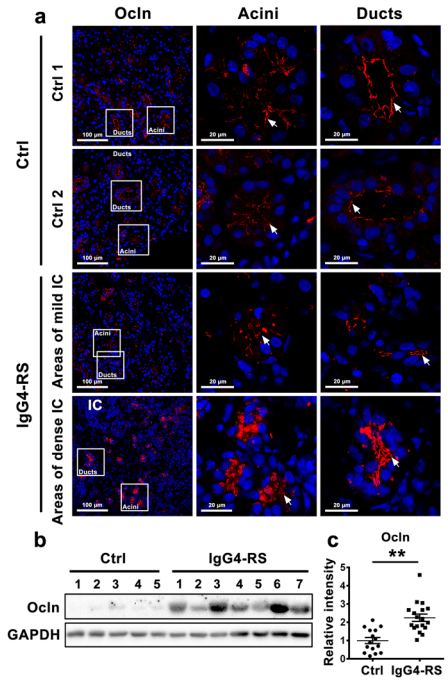

Fig. 6 Distribution and protein expression of occludin in submandibular glands (SMGs) from IgG4-related sialadenitis (IgG4-RS) patients and controls. **a** The immunofluorescence staining of occludin in acini and ducts of SMGs. The areas with mild and dense inflammatory cells infiltrates were both observed in SMGs from IgG4-RS patients. Cell nuclei were stained with DAPI (blue). Arrows pointed to the occludin-specific staining. The enlarged images were derived from the black boxes. *A* acini, *D* duct, *IC* infiltrating cells. **b, c** The protein expression and quantitative analysis of occludin in SMGs from IgG4-RS patients (n = 18) and controls (n = 15). All data are presented as mean ± SEM. *Ctrl* control, *Ocln* occludin. $^{**}P < 0.01$ compared with controls

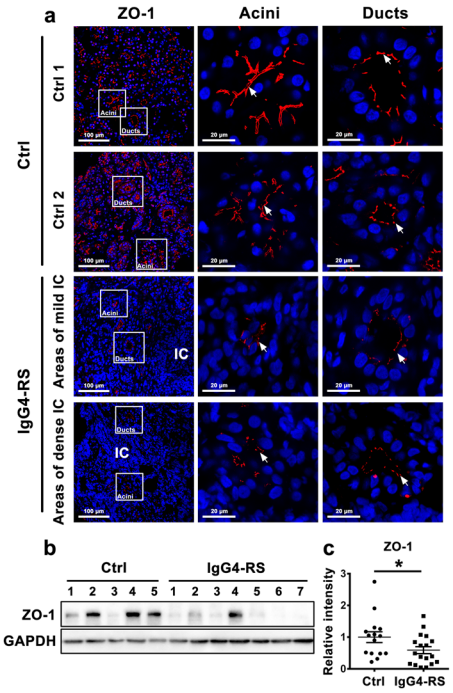

Fig. 7 Distribution and protein expression of zonula occludens-1 (ZO-1) in submandibular glands (SMGs) from IgG4-related sialadenitis (IgG4-RS) patients and controls. **a** The immunofluorescence staining of ZO-1 in acini and ducts of SMGs. The areas with mild and dense inflammatory cells infiltrates were both observed in SMGs from IgG4-RS patients. Cell nuclei were stained with DAPI (blue). Arrows pointed to the ZO-1-specific staining. The enlarged images were derived from the black boxes. *A* acini, *D* duct, *IC* infiltrating cells. **b, c** The protein expression and quantitative analysis of ZO-1 in SMGs from IgG4-RS patients (n = 18) and controls (n = 15). All data are presented as mean ± SEM. *Ctrl* control. $^{**}P < 0.01$ compared with controls

Correlation analysis between TJ protein levels and clinical features

In order to investigate whether TJ abnormalities were associated with secretory dysfunction in IgG4-RS patients, we further analyzed the relationship between TJ protein levels and saliva flow rate as well as serum indexes. The levels of claudin-3 and ZO-1 were positively correlated with saliva flow rate, whereas claudin-1, -4, and occludin contents were not correlated with it (Fig. 8a–e). The elevation of serum concentration of IgG4 is a supplementary indicator for the diagnosis of IgG4-RS (Kawa et al. 2017). Herein, the correlation of TJ protein level and serum IgG4 level was also analyzed, and results showed that none of the TJ protein expressions were statistically correlated with serum IgG4 concentration (Fig. 8f–j). Additionally, an elevated IgE level has often been observed in IgG4-RS patients with allergic history (Li et al. 2015b); however, there was no significant correlation between each TJ protein level and serum IgE concentration (Fig. 8k–o). These results suggested that the alteration of TJ expressions, particularly claudin-3 and ZO-1, might be involved in and reflect the impaired secretory function of IgG4-RS patients.

The change of F-actin arrangement in SMGs from IgG4-RS patients

To further explore the possible mechanisms that affected the TJ structure and function, we focused on the actin cytoskeleton F-actin, which is a direct structural link with TJ complex. In control SMGs, F-actin was dominantly present at the peri-apicolateral membrane regions in acini, and lined along the luminal surface in ducts. However, the distribution of F-actin was discontinued, kinked, and diminished with a dispersed rearrangement pattern in SMGs from IgG4-RS patients. Co-immunofluorescence images showed that F-actin and ZO-1 were co-localized in control SMGs, while in IgG4-RS SMGs, ZO-1 staining was obviously reduced at where the F-actin was disrupted (as arrows shown in Fig. 9). These results indicated that the F-actin architecture was disorganized, which might be responsible for the alteration of TJ proteins observed in SMGs from IgG4-RS patients.

Discussion

In the present study, we demonstrated that the expressions of TJ proteins were markedly altered, characterized by decreased claudin-3, -4, and ZO-1 levels, and increased claudin-1 and occludin levels in SMGs of IgG4-RS patients. Consistently, claudin-1 staining was enhanced and claudin-3, -4 and ZO-1 staining were attenuated at apicolateral membranes, whereas occludin was dispersed into acinar and ductal cytoplasm. Among them, the protein levels of claudin-3 and ZO-1 were positively associated with salivary secretion of IgG4-RS patients. Moreover, we identified that the rearrangement of F-actin may be responsible for the alteration of TJ components in IgG4-RS. These results demonstrate that the impairment of TJ complex, especially claudin-3 and ZO-1, might contribute to the hyposalivation of SMGs in IgG4-RS patients.

IgG4-RD is a systemic chronic disease that can occur in multiple organs and tissues, the salivary glands have received increasing attention in recent years due to the high incidence rate in IgG4-RD patients. In a retrospective study of 428 patients, the salivary glands of 58% IgG4-RD patients are affected. The IgG4-RD patients with the salivary gland lesions are more female and exhibit symptoms at an earlier age and have more organs affected. Moreover, the serum concentration of IgG4 and IgE, as well as IgG4/IgG ratio, are significantly higher than that in the salivary gland-unaffected IgG4-RD patients (Liu et al. 2019). Progressive

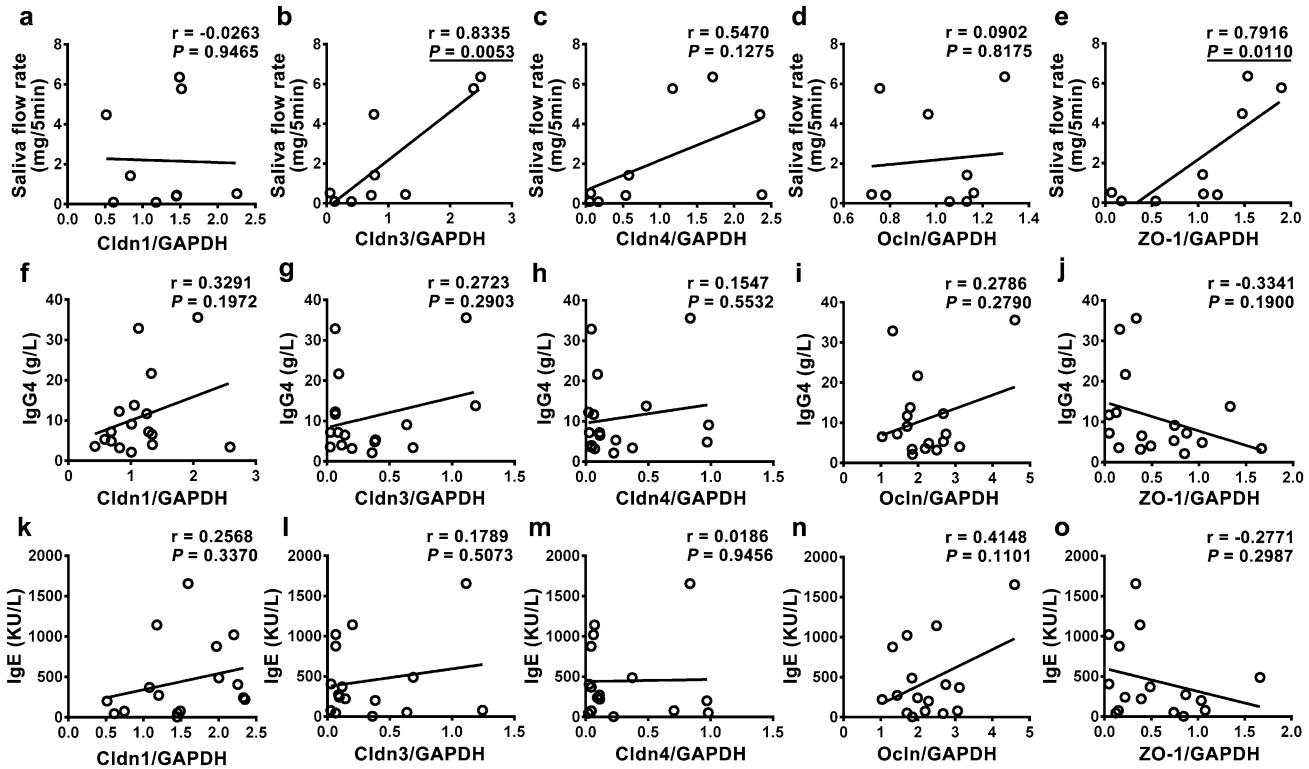

Fig. 8 Correlation analysis between tight junction (TJ) proteins and clinical features in IgG4-related sialadenitis patients. Correlation between TJ proteins in submandibular glands and saliva flow rate (g/5 min, n = 9) (**a–e**), serum IgG4 level (g/L, n = 17) (**f–j**), serum IgE level (KU/L, n = 16) (**k–o**) were analyzed by Pearson's coefficient correlation analysis. *Cldn* claudin, *Ocln* occludin, *ZO-1* zonula occludens-1. $P < 0.05$ was considered statistically significant

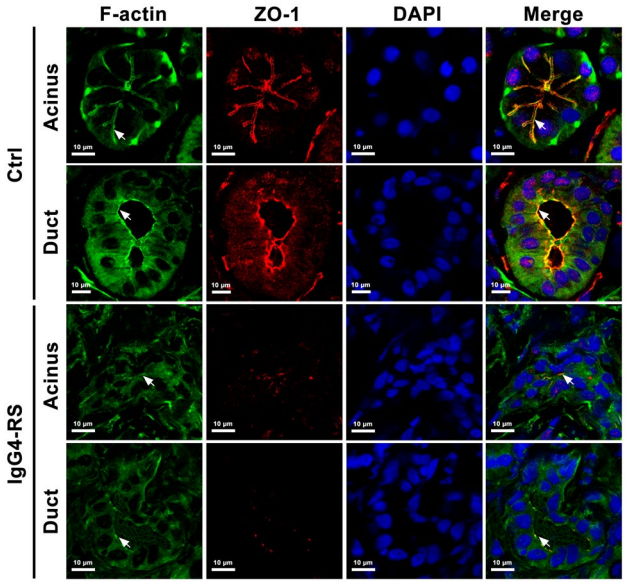

Fig. 9 Distribution of filamentous actin (F-actin) in acini and ducts of submandibular glands from IgG4-related sialadenitis (IgG4-RS) patients and controls. Co-immunofluorescence images showing the localization of F-actin (green) with zonula occludens-1 (red). Cell nuclei were stained with DAPI (blue). Arrows indicated the F-actin staining and the co-staining with zonula occludens-1. *Ctrl* control, *ZO-1* zonula occludens-1

reduction of salivary secretion has been observed in IgG4-RS patients, especially in medium and long-term patients, and early therapeutic interventions are necessary for the retention of salivary gland function (Li et al. 2015b; Moriyama et al. 2013; Shimizu et al. 2013). However, IgG4-RD patients with salivary gland involvement show a longer interval between disease onset and diagnosis (Liu et al. 2019). Therefore, unveiling the pathogenesis of salivary gland hypofunction is valuable for the diagnosis and management of IgG4-RS. In this study, the unstimulated saliva flow rate in 6 of 9 (66.6%) IgG4-RS patients was lower than the normal value (2.05 g/5 min) as we previous measured in 300 healthy subjects (Wang et al. 2015), indicating that the secretory function of salivary gland was declined in IgG4-RS patients. Furthermore, by screening the differential proteins between control and IgG4-RS SMG samples, we found that the identified proteins were enriched in the regulation of actin cytoskeleton and the salivary secretion. Since the actin cytoskeleton is directly linked with ZO-1, which serves as a scaffold protein between the actin cytoskeleton and transmembrane TJs like claudins and occludin, the alteration in the actin cytoskeleton will affect TJ structure and function. Herein, these results point to a possibility that TJ proteins might be involved in the secretory hypofunction of IgG4-RS.

TJs are considered as an indispensable structure to maintain secretory process by regulating the paracellular transport of water, ions, and solutes in SMG epithelium (Baker 2016). It has been found that claudin-1 to -12, occludin, and ZO-1 are expressed in human SMGs (Zhang et al. 2018). Impairment in TJ expression and/or distribution contributes to secretory dysfunction. For example, the absence of claudin-1 results in the disruption of TJ structure and barrier function in rat parotid gland cell line Par-C10 (Baker et al. 2008). Both knockdown of claudin-3 and downregulation of claudin-3 by TNF-α increase the paracellular permeability of rat SMG acinar cell line SMG-C6 (Mei et al. 2015). Claudin-4 knockdown suppresses, whereas claudin-4 overexpression retains the carbachol-induced increased paracellular permeability in SMG-C6 cells (Cong et al. 2015). Occludin also plays an important role in submandibular epithelial cells. Decreased protein level of occludin in salivary glands is observed in both Sjögren's syndrome patients and mouse model (Ewert et al. 2010; Zhang et al. 2016). ZO-1 acts as a scaffolding protein that interacts with transmembrane TJ proteins and actin cytoskeleton like F-actin. In SMG-C6 cells, ZO-1 and -2 single or double knockdown abolished, whereas their rescue restored the capsaicin-induced increase in paracellular permeability (Li et al. 2015a). These above studies demonstrate that the appropriate contents of TJs are crucial determinants for the secretory function of salivary glands through the regulation of paracellular permeability. However, whether TJs are changed in SMGs of IgG4-RS is not fully investigated. Here, we detected the expression of TJ molecules in SMGs at both transcriptional and protein levels. Real-time PCR results showed that the mRNA levels of claudin-3, -4, -6, -7, -8, -10, -12, occludin, and ZO-1 were lower, whereas claudin-1 and -5 were higher in SMGs from IgG4-RS patients compared with those in control SMGs. Consistently, the protein levels of claudin-3, -4, and ZO-1 were significantly decreased, whereas claudin-1 was increased in SMGs of IgG4-RS. However, the protein level of occludin was higher, which was not in accordance with its lower mRNA level. Occludin is a substrate of RING finger protein 186, which is an E3 ubiquitin ligase that regulates protein turnover through degradation. In mice lacking RING finger protein 186, the increased expression of occludin and distribution in cytoplasm are observed in colonic epithelial cells (Fujimoto et al. 2017). Since the ubiquitination is an often-seen modification of occludin, the reason for the inconsistence between mRNA and protein expressions in occludin observed in this study might be a reduction in occludin degradation. These results indicate that the mRNA and protein expression of TJs were dysregulated in SMGs derived from IgG4-RS patients.

Additionally, the appropriate distribution of TJ proteins at the apicolateral plasma membranes guarantees their function in secretion process. Activation of transient receptor potential vanilloid subtype 1 by capsaicin induces redistribution of occludin from cell membranes into the cytoplasm, thereby increasing the paracellular permeability and salivation (Cong et al. 2013). In SMG-C6 cells, the redistribution of ZO-1 and -2 from tight junction complex into the cytoplasm mediate the increased paracellular permeability caused by capsaicin (Li et al. 2015a). In nonobese diabetic mice, claudin-1 and -3 are elevated, and claudin-4 is reduced at the basolateral membranes, whereas occludin and ZO-1 are dispersed into cytoplasm in SMGs, accompanied with a reduction in secretory function (Zhang et al. 2016). In this study, immunohistological and immunofluorescence results showed that the staining of claudin-3, -4 and ZO-1 was significantly reduced, whereas claudin-1 was elevated, particularly at apicolateral membranes of acinar and ductal SMG cells. Notably, as inflammatory cells aggregated, the intensity of claudin-3, -4 and ZO-1, as well as claudin-1, became weaker. Moreover, occludin was dispersed and accumulated in acinar cytoplasm of SMGs in IgG4-RS, together with an increased staining intensity, which was consistent with the higher occludin protein level. These results reveal that TJ components, especially claudin-1, -3, -4, occludin, and ZO-1 are disorganized and loss of them at the apicolateral membranes leads to disrupted barrier function in SMGs from IgG4-RS patients, and moreover, the structure of TJ complex become worse as the severity of lymphocytic infiltration. Therefore, early clinical intervention is necessary for preserving the function of salivary glands involved.

Since abnormalities of TJs organization have often seen in salivary gland inflammatory diseases, there has been an increasing interest in the relationship between exposure to proinflammatory cytokines and loss of barrier function. In SMG-C6, TNF-α disrupts epithelial barrier by selectively downregulating claudin-3 through ERK1/2/slug signaling axis (Mei et al. 2015). After exposure to TNF-α and IFN-γ, occludin is redistributed from apical to lateral and basal membranes in acini isolated from human SMGs, but the staining intensity of occludin is dramatically reduced (Ewert et al. 2010). In Sjögren's syndrome mouse model, proinflammatory cytokine IL-17 is increased in SMGs and impairs salivary TJ integrity by reducing claudin-4 and ZO-1 through NF-κB signaling pathway (Zhang et al. 2016). Recent studies have shown that the accumulation of immune cells including Th1, Th2, regulatory T, cytotoxic $CD4^+$ T, follicular helper T cells, and macrophages in IgG4-RS lesions are involved in the pathogenesis of IgG4-RS by releasing cytokines, such as IL-4, IL-10, IL-17, TGF-β, TNF-α, and IFN-γ, leading to acinar cell injury and fibrosis (Hong et al. 2019; Maehara et al. 2017; Ohta et al. 2012; Takeuchi et al. 2014). Here, we performed KEGG pathway analysis and found that differentially expressed proteins were enriched in inflammation related pathways. Moreover, the loss of TJ expressions and distribution were worse in areas

with high inflammation and fibrosis grade. These results suggest that the local inflammatory microenvironment might be responsible for TJ impairment in IgG4-RS patients.

In constituting a complicated TJ complex, each TJ component has its own role and contribution to the integrity and function of TJs. Hence, the changes in the expression and/or distribution of TJ molecules would have impacts on TJ function. However, it should be noted that the importance of each TJ component might be different. For example, in renal proximal tubule, claudin-2, claudin-10a and claudin-17 serve as paracellular channel formers involved in the resorption of cations, anions, or water, while claudin-11, occludin, and tricellulin function as barrier formers against leaky passage of nutrients and larger molecules (Fromm et al. 2017). Therefore, to clarify the contribution of salivary TJs to hyposalivation in IgG4-RS patients, the relationship between TJ protein expression levels and saliva flow rate in patients were further analyzed. The saliva flow rate was positively correlated with claudin-3 and ZO-1, but not claudin-1, -4, or occludin. Claudin-3, which plays a crucial role in the barrier function of epithelial cells, is strongly associated with local inflammation (Garcia-Hernandez et al. 2017). In SMG epithelium, claudin-3 is the specific target regulated by TNF-α (Mei et al. 2015). Mice that lack claudin-3 exhibits dedifferentiated and leaky colonic epithelium and the loss of claudin-3 in colonic epithelium activates glycoprotein130/interleukin-6/signal transducer and activator of transcription 3 signaling, leading to colon cancer progression (Ahmad et al. 2017). ZO-1 is a cytosolic TJ-associated protein that determines TJ assembly, and deficiency of ZO-1 is associated with barrier dysfunction in many diseases including inflammatory bowel disease, dermatitis, and cerebral ischemia (Wei et al. 2017; Basler and Brandner 2017; Reinhold and Rittner 2017). In patients with inactive Crohn's disease, ZO-1 is dislocated from apical to basolateral membrane in intestinal mucosa (Ohira et al. 2009). In mouse model of dextran sulfate sodium-induced colitis, the loss of ZO-1 in colonic mucosa occurs before intestinal inflammation, followed by an increase in permeability (Poritz et al. 2007). In db/db mice, ZO-1 expression is reduced in the intestinal epithelium, and the microbial anti-inflammatory molecule from *Faecalibacterium prausnitzii* can restore the intestinal barrier structure and function by upregulating ZO-1 expression (Xu et al. 2019). Here, our results that showed the positive relationship between the saliva flow rate and the protein levels of claudin-3 and ZO-1, but not claudin-1, -4, or occludin, further suggest that the abnormal expression of claudin-3 and ZO-1 might be the major cause of secretory dysfunction in IgG4-RS patients. Due to limited sample size in this study, more studies are required to verify the pathogenic role of TJ complex impairment in IgG4-RS progression in the future.

Furthermore, the possible mechanism that was involved in the impairment of TJs in SMGs of IgG4-RS patients was explored. F-actin is a crucial actin cytoskeleton involved in the regulation of TJ complex formation and function. For example, proteomic analysis of human transplanted long-term SMGs shows that cytoskeletal proteins are all upregulated, and the decrease of F-actin at the peri-apicolateral membranes is involved in hypersecretion of patients (Ding et al. 2011). In the process of lumenogenesis, the direct link with F-actin through actin binding region is required for ZO-1 to regulate epithelial polarization (Odenwald et al. 2017). In diabetic mice, elevated pigment epithelium-derived factor aggravates proteinuria by inducing podocyte F-actin rearrangement and ZO-1 reduction (Huang et al. 2019). In intestinal epithelial cells, induction of myosin light chain kinase causes myosin light chain phosphorylation and increases TJ permeability by inducing separation of ZO-1 and occludin from F-actin (Shen et al. 2006). In the present study, F-actin architecture became disorganized with a significant decrease at peri-apicolateral membranes in both acinar and ductal cells of SMGs from IgG4-RS patients, at where ZO-1 that mediates the anchoring of actin filaments was also disappeared. These results suggest that the rearrangement of F-actin might be responsible for the alteration of TJ distribution in IgG4-RS and provide more evidence for the involvement of ZO-1 in IgG4-RS pathogenesis.

Notably, IgG4-RD can develop or coexist with other systemic autoimmune diseases such as rheumatoid arthritis and systemic lupus erythematosus (Soliotis et al. 2014). The accumulation of $CD4^+$ cytotoxic T lymphocytes is found both in lesions of IgG4-RD and other autoimmune conditions (Maehara et al. 2017; Thewissen et al. 2007). The levels of serum IgG4 are also elevated in some patients with rheumatoid arthritis and systemic sclerosis (Yamamoto et al. 2012). These findings suggest that IgG4-RD might be associated with autoimmune diseases due to the shared underlying pathogenetic mechanisms. Therefore, autoimmune disorders have been considered as potential contributors to IgG4-RD. Although these comorbidities have been found in IgG4-RD patients, little is known about the exact effects of allergic and autoimmune disorders on secretory function of salivary gland in IgG4-RD patients. More efforts should be made on this important issue in the future.

In summary, we demonstrate that TJ composition and organization are impaired in SMGs from IgG4-RS patients, which contribute to hyposalivation occurred in IgG4-RS patients. The reorganization of F-actin might be involved in the disruption of TJ structure in SMG epithelium of IgG4-RS patients. These findings provide new insights for the pathogenesis of IgG4-RS, and a more thorough understanding on TJ proteins will facilitate the diagnosis and development of treatment regimens for IgG4-RS.

Acknowledgements This work was funded by the National Natural Science Foundation of China 81671005 (GYY), 81974151 (GYY), and 81771093 (XC).

Author contributions SNM performed the major experiments and wrote the manuscript. YYZ and WXZ were responsible for the collection of clinical data. LLW participated in data interpretation and wrote the manuscript. XC and GYY designed the study, analyzed the data, and wrote the manuscript. All authors read and approved the final manuscript.

Compliance with ethical standards

Conflict of interest The authors have no conflicts of interest to disclose.

References

Abe A, Takano K, Kojima T, Nomura K, Kakuki T, Kaneko Y, Yamamoto M, Takahashi H, Himi T (2016) Interferon-gamma increased epithelial barrier function via upregulating claudin-7 expression in human submandibular gland duct epithelium. J Mol Histol 47:353–363. https://doi.org/10.1007/s10735-016-9667-2

Ahmad R, Kumar B, Chen Z et al (2017) Loss of claudin-3 expression induces IL6/gp130/Stat3 signaling to promote colon cancer malignancy by hyperactivating Wnt/β-catenin signaling. Oncogene 36:6592–6604. https://doi.org/10.1038/onc.2017.259

Baker OJ (2016) Current trends in salivary gland tight junctions. Tissue Barriers 4:e1162348. https://doi.org/10.1080/21688370.2016.1162348

Baker OJ, Camden JM, Redman RS, Jones JE, Seye CI, Erb L, Weisman GA (2008) Proinflammatory cytokines tumor necrosis factor-alpha and interferon-gamma alter tight junction structure and function in the rat parotid gland Par-C10 cell line. Am J Physiol Cell Physiol 295:C1191–C1201. https://doi.org/10.1152/ajpcell.00144.2008

Barrera MJ, Bahamondes V, Sepúlveda D et al (2013) Sjogren's syndrome and the epithelial target: a comprehensive review. J Autoimmun 42:7–18. https://doi.org/10.1016/j.jaut.2013.02.001

Basler K, Brandner JM (2017) Tight junctions in skin inflammation. Pflugers Arch 469:3–14. https://doi.org/10.1007/s00424-016-1903-9

Brito-Zeron P, Ramos-Casals M, Bosch X, Stone JH (2014) The clinical spectrum of IgG4-related disease. Autoimmun Rev 13:1203–1210. https://doi.org/10.1016/j.autrev.2014.08.013

Buckley A, Turner JR (2018) Cell biology of tight junction barrier regulation and mucosal disease. Cold Spring Harb Perspect Biol 10:a029314. https://doi.org/10.1101/cshperspect.a029314

Cong X, Zhang Y, Yang NY et al (2013) Occludin is required for TRPV1-modulated paracellular permeability in the submandibular gland. J Cell Sci 126:1109–1121. https://doi.org/10.1242/jcs.111781

Cong X, Zhang Y, Li J et al (2015) Claudin-4 is required for modulation of paracellular permeability by muscarinic acetylcholine receptor in epithelial cells. J Cell Sci 128:2271–2286. https://doi.org/10.1242/jcs.165878

Ding C, Zhang Y, Peng X et al (2011) Proteomic analysis of human transplanted submandibular gland in patients with epiphora after transplantation. J Proteome Res 10:2206–2215. https://doi.org/10.1021/pr100965q

Ding C, Cong X, Zhang XM, Li SL, Wu LL, Yu GY (2017) Decreased interaction between ZO-1 and occludin is involved in alteration of tight junctions in transplanted epiphora submandibular glands. J Mol Histol 48:225–234. https://doi.org/10.1007/s10735-017-9716-5

Ewert P, Aguilera S, Alliende C et al (2010) Disruption of tight junction structure in salivary glands from Sjogren's syndrome patients is linked to proinflammatory cytokine exposure. Arthritis Rheum 62:1280–1289. https://doi.org/10.1002/art.27362

Forster C (2008) Tight junctions and the modulation of barrier function in disease. Histochem Cell Biol 130:55–70. https://doi.org/10.1007/s00418-008-0424-9

Fromm M, Piontek J, Rosenthal R, Gunzel D, Krug SM (2017) Tight junctions of the proximal tubule and their channel proteins. Pflugers Arch 469:877–887. https://doi.org/10.1007/s00424-017-2001-3

Fujimoto K, Kinoshita M, Tanaka H et al (2017) Regulation of intestinal homeostasis by the ulcerative colitis-associated gene RNF186. Mucosal Immunol 10:446–459. https://doi.org/10.1038/mi.2016.58

Garcia-Hernandez V, Quiros M, Nusrat A (2017) Intestinal epithelial claudins: expression and regulation in homeostasis and inflammation. Ann N Y Acad Sci 1397:66–79. https://doi.org/10.1111/nyas.13360

Hong X, Min SN, Zhang YY, Lin YT, Wang F, Huang Y, Yu GY, Wu LL, Yang HY (2019) TNF-α suppresses autophagic flux in acinar cells in IgG4-related sialadenitis. J Dent Res 98:1386–1396. https://doi.org/10.1177/0022034519871890

Huang N, Zhang X, Jiang Y, Mei H, Zhang L, Zhang Q, Hu J, Chen B (2019) Increased levels of serum pigment epithelium-derived factor aggravate proteinuria via induction of podocyte actin rearrangement. Int Urol Nephrol 51:359–367. https://doi.org/10.1007/s11255-018-2026-3

Kawa S, Skold M, Ramsden DB, Parker A, Harding SJ (2017) Serum IgG4 concentration in IgG4-related disease. Clin Lab 63:1323–1337. https://doi.org/10.7754/Clin.Lab.2017.170403

Krug SM, Schulzke JD, Fromm M (2014) Tight junction, selective permeability, and related diseases. Semin Cell Dev Biol 36:166–176. https://doi.org/10.1016/j.semcdb.2014.09.002

Li J, Cong X, Zhang Y et al (2015a) ZO-1 and -2 are required for TRPV1-modulated paracellular permeability. J Dent Res 94:1748–1756. https://doi.org/10.1177/0022034515609268

Li W, Chen Y, Sun ZP et al (2015b) Clinicopathological characteristics of immunoglobulin G4-related sialadenitis. Arthritis Res Ther 17:186. https://doi.org/10.1186/s13075-015-0698-y

Liu Y, Xue M, Wang Z et al (2019) Salivary gland involvement disparities in clinical characteristics of IgG4-related disease: a retrospective study of 428 patients. Rheumatology (Oxford). https://doi.org/10.1093/rheumatology/kez280

Maehara T, Mattoo H, Ohta M et al (2017) Lesional $CD4^+$ IFN-γ^+ cytotoxic T lymphocytes in IgG4-related dacryoadenitis and sialoadenitis. Ann Rheum Dis 76:377–385. https://doi.org/10.1136/annrheumdis-2016-209139

Mei M, Xiang RL, Cong X et al (2015) Claudin-3 is required for modulation of paracellular permeability by TNF-α through ERK1/2/slug signaling axis in submandibular gland. Cell Signal 27:1915–1927. https://doi.org/10.1016/j.cellsig.2015.07.002

Moriyama M, Tanaka A, Maehara T et al (2013) Clinical characteristics of Mikulicz's disease as an IgG4-related disease. Clin Oral Investig 17:1995–2002. https://doi.org/10.1007/s00784-012-0905-z

Muller T, Beutler C, Pico AH et al (2013) Increased T-helper 2 cytokines in bile from patients with IgG4-related cholangitis disrupt the tight junction-associated biliary epithelial cell barrier. Gastroenterology 144:1116–1128. https://doi.org/10.1053/j.gastro.2013.01.055

Nam K, Maruyama CL, Trump BG, Buchmann L, Hunt JP, Monroe MM, Baker OJ (2016) Post-irradiated human submandibular glands display high collagen deposition, disorganized cell junctions, and an increased number of adipocytes. J Histochem

Cytochem 64:343–352. https://doi.org/10.1369/0022155416646089

Odenwald MA, Choi W, Buckley A et al (2017) ZO-1 interactions with F-actin and occludin direct epithelial polarization and single lumen specification in 3D culture. J Cell Sci 130:243–259. https://doi.org/10.1242/jcs.188185

Ohira M, Oshitani N, Hosomi S et al (2009) Dislocation of Rab13 and vasodilator-stimulated phosphoprotein in inactive colon epithelium in patients with Crohn's disease. Int J Mol Med 24:829–835. https://doi.org/10.3892/ijmm_00000300

Ohta N, Makihara S, Okano M et al (2012) Roles of IL-17, Th1, and Tc1 cells in patients with IgG4-related sclerosing sialadenitis. Laryngoscope 122:2169–2174. https://doi.org/10.1002/lary.23429

Poritz LS, Garver KI, Green C, Fitzpatrick L, Ruggiero F, Koltun WA (2007) Loss of the tight junction protein ZO-1 in dextran sulfate sodium induced colitis. J Surg Res 140:12–19. https://doi.org/10.1016/j.jss.2006.07.050

Reinhold AK, Rittner HL (2017) Barrier function in the peripheral and central nervous system-a review. Pflugers Arch 469:123–134. https://doi.org/10.1007/s00424-016-1920-8

Shen L, Black ED, Witkowski ED, Lencer WI, Guerriero V, Schneeberger EE, Turner JR (2006) Myosin light chain phosphorylation regulates barrier function by remodeling tight junction structure. J Cell Sci 119:2095–2106. https://doi.org/10.1242/jcs.02915

Shimizu Y, Yamamoto M, Naishiro Y et al (2013) Necessity of early intervention for IgG4-related disease-delayed treatment induces fibrosis progression. Rheumatology (Oxford) 52:679–683. https://doi.org/10.1093/rheumatology/kes358

Soliotis F, Mavragani CP, Plastiras SC, Rontogianni D, Skopouli FN, Moutsopoulos HM (2014) IgG4-related disease: a rheumatologist's perspective. Clin Exp Rheumatol 32:724–727

Stone JH, Zen Y, Deshpande V (2012) IgG4-related disease. N Engl J Med 366:539–551. https://doi.org/10.1056/NEJMra1104650

Takeuchi M, Sato Y, Ohno K et al (2014) T helper 2 and regulatory T-cell cytokine production by mast cells: a key factor in the pathogenesis of IgG4-related disease. Mod Pathol 27:1126–1136. https://doi.org/10.1038/modpathol.2013.236

Thewissen M, Somers V, Hellings N, Fraussen J, Damoiseaux J, Stinissen P (2007) $CD4^{+}CD28$null T cells in autoimmune disease: pathogenic features and decreased susceptibility to immunoregulation. J Immunol 179:6514–6523. https://doi.org/10.4049/jimmunol.179.10.6514

Umehara H, Okazaki K, Masaki Y et al (2012) Comprehensive diagnostic criteria for IgG4-related disease (IgG4-RD), 2011. Mod Rheumatol 22:21–30. https://doi.org/10.1007/s10165-011-0571-z

Umehara H, Nakajima A, Nakamura T, Kawanami T, Tanaka M, Dong L, Kawano M (2014) IgG4-related disease and its pathogenesis-cross-talk between innate and acquired immunity. Int Immunol 26:585–595. https://doi.org/10.1093/intimm/dxu074

Wang Z, Shen MM, Liu XJ, Si Y, Yu GY (2015) Characteristics of the saliva flow rates of minor salivary glands in healthy people. Arch Oral Biol 60:385–392. https://doi.org/10.1016/j.archoralbio.2014.11.016

Wei SC, Yang-Yen HF, Tsao PN et al (2017) SHANK3 regulates intestinal barrier function through modulating ZO-1 expression through the PKCε-dependent pathway. Inflamm Bowel Dis 23:1730–1740. https://doi.org/10.1097/mib.0000000000001250

Xu J, Liang R, Zhang W, Tian K, Li J, Chen X, Tao Y, Chen Q (2019) Faecalibacterium prausnitzii-derived Microbial Anti-inflammatory Molecule regulates intestinal integrity in diabetes mellitus mice via modulating tight junction protein expression. J Diabetes. https://doi.org/10.1111/1753-0407.12986

Yamamoto M, Tabeya T, Naishiro Y et al (2012) Value of serum IgG4 in the diagnosis of IgG4-related disease and in differentiation from rheumatic diseases and other diseases. Mod Rheumatol 22:419–425. https://doi.org/10.1007/s10165-011-0532-6

Yang NY, Ding C, Li J, Zhang Y, Xiang RL, Wu LL, Yu GY, Cong X (2017) Muscarinic acetylcholine receptor-mediated tight junction opening is involved in epiphora in late phase of submandibular gland transplantation. J Mol Histol 48:99–111. https://doi.org/10.1007/s10735-016-9709-9

Zhang GH, Wu LL, Yu GY (2013) Tight junctions and paracellular fluid and ion transport in salivary glands. Chin J Dent Res 16:13–46

Zhang LW, Cong X, Zhang Y et al (2016) Interleukin-17 impairs salivary tight junction integrity in Sjogren's syndrome. J Dent Res 95:784–792. https://doi.org/10.1177/0022034516634647

Zhang XM, Huang Y, Zhang K, Qu LH, Cong X, Su JZ, Wu LL, Yu GY, Zhang Y (2018) Expression patterns of tight junction proteins in porcine major salivary glands: a comparison study with human and murine glands. J Anat 233:167–176. https://doi.org/10.1111/joa.12833